TÜBİTAK

Turkish Journal of Physics

http://journals.tubitak.gov.tr/physics/

Research Article

Turk J Phys
(2013) 37: 113 – 120

doi:10.3906/fiz-1202-7

Study of solid-state stability of the ZOTO binary system

Sandeep Anandrao WAGHULEY*
Department of Physics, Sant Gadge Baba Amravati University, Amravati 444602, India

Received: 05.02.2012 • **Accepted:** 10.09.2012 • **Published Online:** 20.03.2013 • **Printed:** 22.04.2013

Abstract: The ZOTO binary system contains different compositions of zinc oxide (ZnO) and tin oxide (SnO_2). These are important semiconductors and have been intensively explored for various applications. SnO_2, ZnO, and different mole ratios (70:30, 40:60, 30:70, and 20:80 SnO_2:ZnO) of the ZOTO system were prepared through proper thermal treatment in powder form. The comparative solid-state stability was investigated using thermogravimetric and differential thermal analysis (TG-DTA). The stability study showed that the SnO_2 material absorbs much lower heat (Ea = –72.06 kJ/g mol) compared with ZnO and their compositions. Thus the SnO_2 material shows stability at near room temperature operation. The crystallite size of the materials was estimated using XRD analysis.

Key words: Solid state stability, ZnO, SnO_2, ZOTO binary system

1. Introduction

Nowadays, transparent conducting oxides (TCOs) have attracted great attention due to their potential application in solar cells [1,2] and advanced optoelectronic devices, like flexible displays [3,4], and catalytic activity [5]. Minami et al. [6] reported the stability of a number of TCO films prepared by magnetron sputtering. The SnO_2 shows platelet-like morphology, which might be because of the crystal growth of SnO_2 toward the reflection planes of a tetragonal lattice, which limits the size to ball-like morphology under low pressure [7].

Cetinorgu et al. [8] investigated the highly transparent Sn doped, ZnO thin films deposited with FVAD, utilizing its high deposition rate. In their investigation, the optical properties of the films, including optical band gap, absorption coefficient, and the complex refractive index (real and imaginary parts), were calculated by applying a single oscillator model to the transmission data and ellipsometry data. The films that were deposited on glass had a maximum transmission of about 90%. The optical band gap was in the range 3.54–3.62 eV. The refractive index and the extinction coefficient derived from spectroscopic ellipsometry decreased with the wavelength from 2.37 to 1.97 and from 0.24 to 0.013, respectively.

Zheng et al. [9] studied a network-structured SnO_2/ZnO heterojunction nanocatalyst with high photocatalytic activity that was successfully synthesized through a simple 2-step solvothermal method.

Thermogravimetric analysis (TGA) is a thermal analysis technique that measures the weight change in a material as a function of temperature and time, in a controlled environment. Differential thermal analysis (DTA) is a calorimetric technique, recording the temperature and heat flow associated with thermal transitions in a material. The TGA for thermal stability and durability is a good technique [10,11] and can be useful for evaluating kinetics parameters at various reactions and materials.

*Correspondence: sandeepwaghuley@sgbau.ac.in

In the light of the above scientific importance, the present work deals with the solid-state stability study of SnO_2, ZnO, and ZOTO of binary system (SnO_2:ZnO compositions) using TG-DTA.

2. Experimental

The analytical reagent grade metal oxides in powder form SnO_2 and ZnO were used in the present work. They were calcined at 800 °C in an automatically temperature controlled muffle furnace (Gallenkamp, UK) for 4 to 5 h. The powder of these materials was mixed with a pestle and mortar before and after calcinations to form fine homogeneous powder.

The powders of mole percentage ratios of 80:20, 70:30, 60:40, 50:50, 40:60, 30:70, and 20:80 of SnO_2:ZnO were mixed together thoroughly in acetone to form a homogeneous mixture of both. After mixing, the mixed powders were subjected to heating at 800 °C for 1 h. In this way, powders of pure materials and their composites of SnO_2 and ZnO were prepared.

TG-DTA characterization was carried out by simultaneous TG-DTA under an inert atmosphere as shown in Figure 1. The reference was an empty aluminum pan, and the flow of argon was set at 200 mL min^{-1}. A small amount of material (3–9 mg) was placed in a sample aluminum pan. The temperature scan was from room temperature (RT) to 900 °C and the heating rate was set at 10 °C min^{-1}.

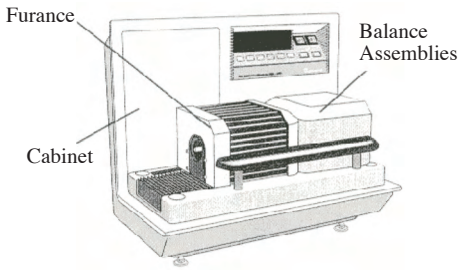

Figure 1. Simultaneous TG-DTA system.

The XRD pattern was recorded on a Philips-1730 (PANalytical) X-ray diffractometer using a CuKα source (λ = 1.54 Å). The diffractogram was in the term of 2θ at continuous scan type at step size 2θ = 0.0170°.

3. Results and discussion

Figures 2a and b show the TG-DTA plots and simultaneously recorded derivative of DTA (DDTA) curves of SnO_2 material. A significant loss of weight is observed from RT to 550 °C without a plateau, with a loss of about 5.2%. The total rate of decomposition is found to be 0.466 × 10^{-3} mg/°C and total loss is 5.74%. The DTA data show an endothermic peak at 38 °C associated with surface water loss and a small exothermic peak at 495 °C. The exothermic peak may be attributed to phase change.

If the DTA curve and its derivative (DDTA) are simultaneously recorded, the 2 inflection points, i.e. the maximum and the minimum slopes of the DTA peak corresponding to the maximum and the minimum of the DDTA double peak, are obtained [12]. Therefore, the temperatures T_{f1} and T_{f2} can be easily and exactly detected on the DDTA curve.

The temperatures of the double peak, T_{f1} = 61 °C and T_{f2} = 38 °C, on the DDTA curve (Figure 2b) for the endothermic peak of the DTA curve (Figure 2a) are observed. Similarly, for the exothermic peak, T_{f1} = 495 °C and T_{f2} = 525 °C are observed for SnO_2.

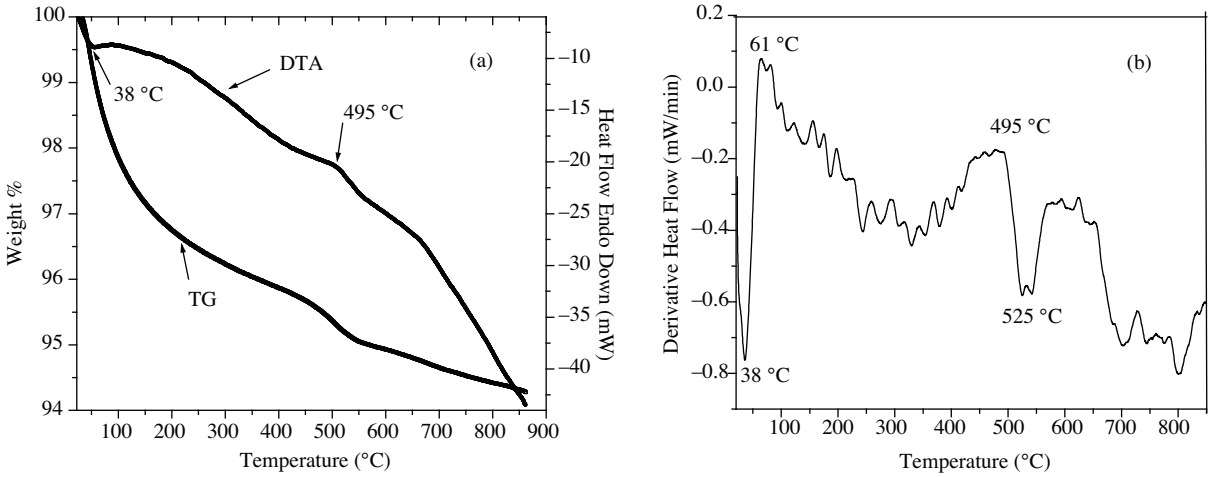

Figure 2. TG-DTA plots of SnO_2 (a) and (b) simultaneously recorded DDTA curve.

The activation energy (E_a) of the first order reaction (n =1) using temperatures of the 2 inflection points T_{f1} and T_{f2} can be derived from Eq. (1) [13]:

$$\frac{E_a}{R}\left(\frac{1}{T_{f1}}-\frac{1}{T_{f2}}\right) = 1.92 \tag{1}$$

where R is the gas constant (8.31 J/g mol K).

For ZnO, a continuous weight loss from RT to 850 °C is observed on the TGA curve (Figure 3a). An endothermic peak on the DTA curve (Figure 3a) is observed at 46 °C, which corresponds to loss of surface water. The small exothermic peak at 598 °C (Figure 3a) may be attributed to phase change. The observed total rate of decomposition and total loss for ZnO are 0.954×10^{-3} mg/°C and 7.2%, respectively. The detected temperatures of inflection points for endothermic and exothermic peaks are shown in Figure 3b.

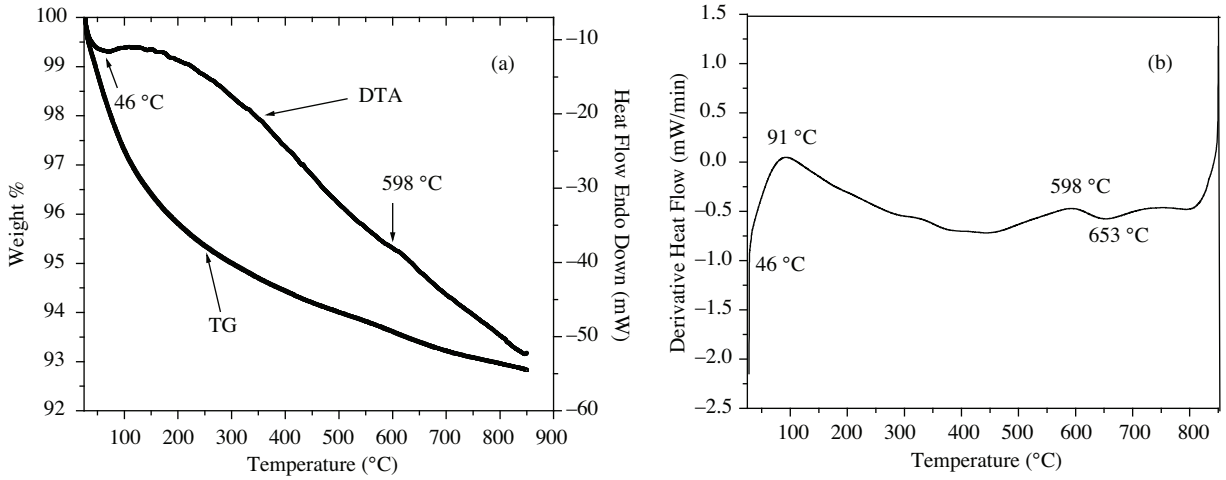

Figure 3. TG-DTA plots of ZnO (a) and (b) simultaneously recorded DDTA curve.

Figures 4a and b show TG-DTA curves and DDTA curve of composite $20SnO_2$:80ZnO material. A continuous weight loss from RT to 850 °C is observed on the TGA curve for this material also. The DTA

curve shows the endothermic peak at 43 °C and an exothermic peak is not observed. The corresponding temperatures of inflection points to endothermic peak are detected on the DDTA curve (Figure 4b). The total rate of decomposition and total loss are 0.953 × 10^{-3} mg/°C and 6.4%, respectively, for this composite.

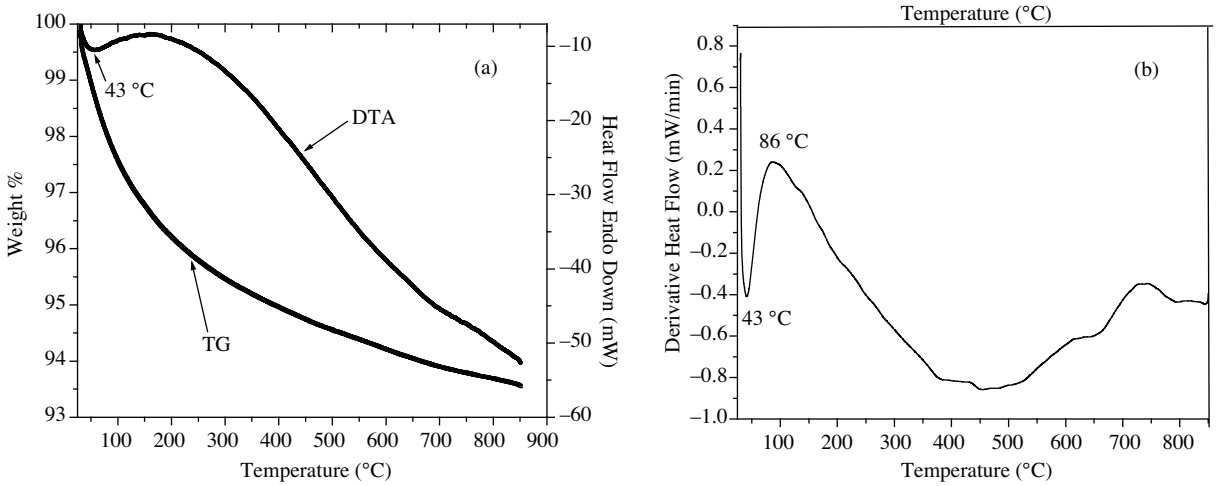

Figure 4. TG-DTA plots of composite 20SnO_2:80ZnO (a) and (b) simultaneously recorded DDTA curve.

Figures 5a and b show the TG-DTA curves and DDTA curve of composite 30SnO_2:70ZnO material. In this composition also is observed continuous weight loss from RT to 850 °C on the TGA curve. An exothermic peak is not observed and an endothermic peak is seen at 39.5 °C. The DDTA curve (Figure 5b) shows the inflection point temperatures corresponding to the endothermic peak on the DTA curve. The total rate of decomposition and total loss are 1.29 × 10^{-3} mg/°C and 9.6%, respectively, for this composite.

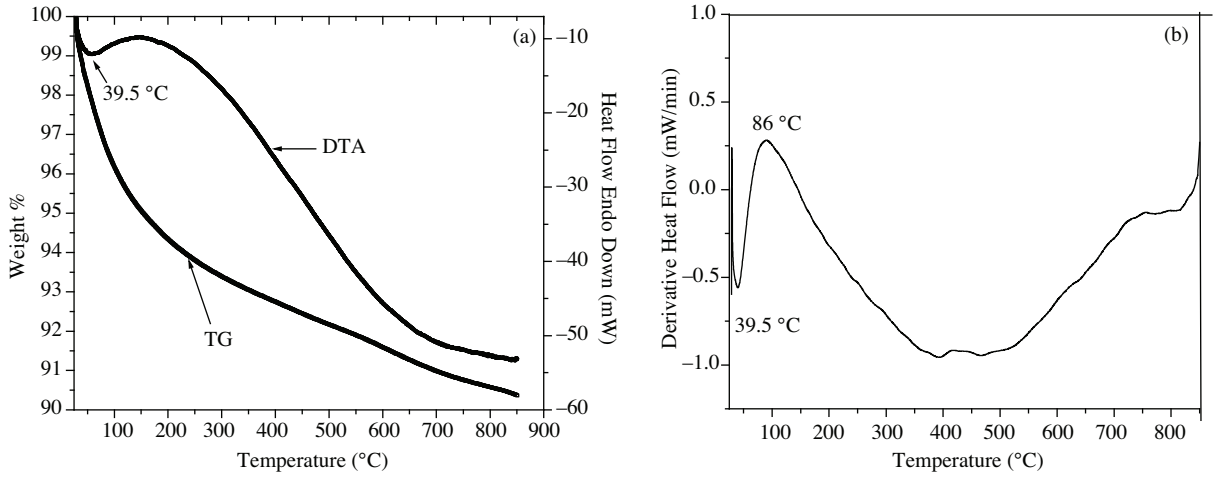

Figure 5. TG-DTA plots of composite 30SnO_2:70ZnO (a) and (b) simultaneously recorded DDTA curve.

For composition 40SnO_2:60ZnO, continuous weight loss is observed on the TGA curve (Figure 6a). An endothermic peak at 42 °C on the DTA curve (Figure 6a) and corresponding inflection point temperatures on the DDTA curve (Figure 6b) are found. An exothermic peak for this composition is observed at 621 °C on the DTA curve, which may be attributed to phase change. The total rate of decomposition is 1.003 × 10^{-3} mg/°C and total loss is 6.6%.

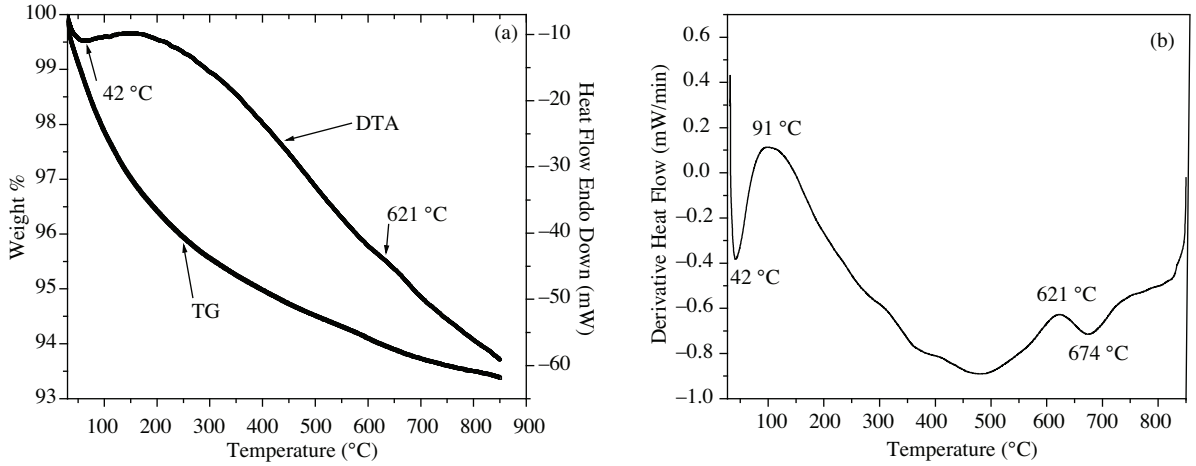

Figure 6. TG-DTA plots of composite $40SnO_2$:60ZnO (a) and (b) simultaneously recorded DDTA curve.

For composition $70SnO_2$:30ZnO, a continuous weight loss on TGA and a small endothermic peak at 41 °C on DTA (Figure 7a) are observed. The temperatures of inflection point correspond to an endothermic peak on the DDTA curve (Figure 7b). An exothermic peak on DTA for this composition is not observed. The total rate of decomposition and total loss are 1.069×10^{-3} mg/°C and 7%.

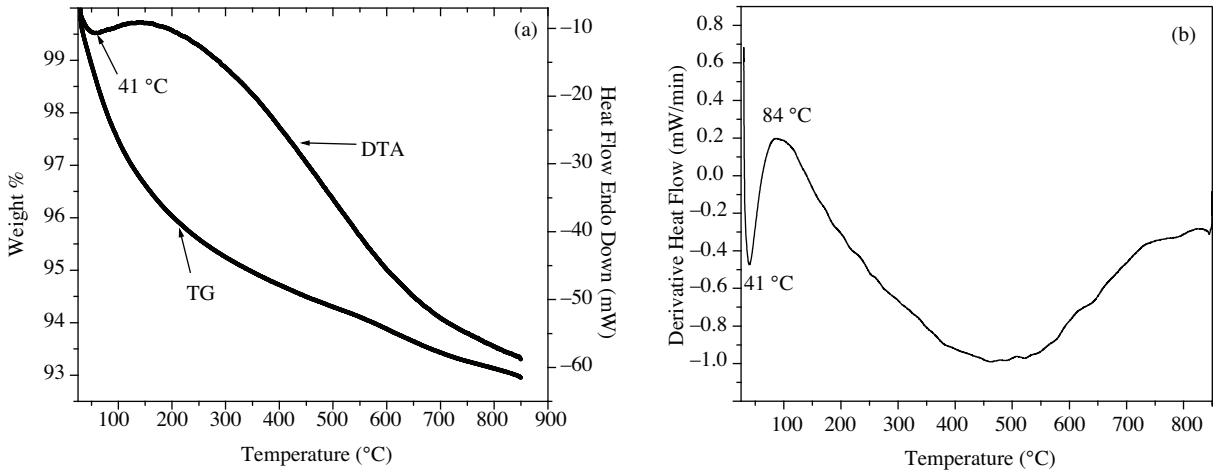

Figure 7. TG-DTA plots of composite $70SnO_2$:30ZnO (a) and (b) simultaneously recorded DDTA curve.

The endothermic peaks observed in these compositions at 43 °C (Figure 4a), 39.5 °C (Figure 5a), 42 °C (Figure 6a), and 41 °C (Figure 7a) correspond to loss of water molecules, which indicates the hydrated form of $ZnO \cdot H_2O$ and $SnO_2 \cdot H_2O$ [14].

Activation energy (E_g) for endothermic and exothermic peaks on DTA, detected as a double peak on DDTA, is calculated from Eq. (1) and listed in Table 1.

The SnO_2 material absorbs much lower heat (E_a = –72.06 kJ/g mol) compared with ZnO and their compositions. Thus the SnO_2 material shows solid-state stability at near room temperature operation.

The X-ray powder diffraction patterns of SnO_2, ZnO, and their compositions calcined at 800 °C for 4–5 h were recorded in terms of 2θ in the range 10–100° and are shown in Figures 8a to f. The prominent peaks

Table 1. Activation energies of SnO_2, ZnO, and their compositions.

Chemical composition SnO_2:ZnO	Double peak temperature of heat endo (°C)		Double peak temperature of heat exo (°C)		Activation energy from endo DDTA E_g (kJ/g mol)	Activation energy from exo DDTA E_g (kJ/g mol)
	T_{f1}	T_{f2}	T_{f1}	T_{f2}		
SnO_2	61	38	495	528	72.06	325.95
ZnO	91	46	598	653	40.39	233.97
$20SnO_2$:80ZnO	86	43	-	-	42.09	-
$30SnO_2$:70ZnO	86	39.5	-	-	38.49	-
$40SnO_2$:60ZnO	91	42	621	674	37.34	254.87
$70SnO_2$:30ZnO	84	41	-	-	41.59	-

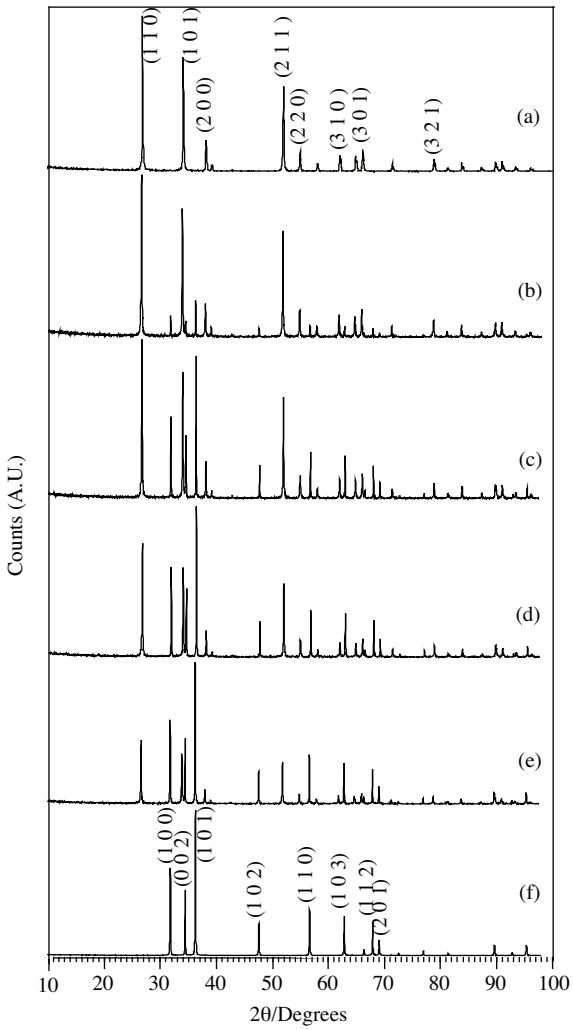

Figure 8. X-ray powder diffraction patterns of (a) SnO_2, (b) $70SnO_2$:30ZnO, (c) $40SnO_2$:60ZnO, (d) $30SnO_2$:70ZnO, (e) $20SnO_2$:80ZnO, (f) ZnO.

observed in the XRD spectra are due to SnO_2 and ZnO. The intensity of the peaks varies with SnO_2 and ZnO concentration. The (h k l) values are calculated for various peaks in the XRD spectra. SnO_2 (tetragonal) has one stable state called cassiterite and ZnO (hexagonal) crystallizes in a wurtzite structure [15,16]. The lattice parameter values obtained for SnO_2 are a = b = 4.7374 Å and c = 3.1864 Å with a c/a ratio of 0.6726 and for ZnO are a = b = 3.249 Å and c = 5.201 Å with a c/a ratio of 1.6, respectively [17]. These values are in good agreement with the values reported in the literature [18,19]. The crystallite size (D) calculated from Scherrer's formula [20] using FWHM is listed in Table 2. The SnO_2 material shows a smaller crystallite size compared with ZnO and their compositions.

Table 2. The values of crystallite size of SnO_2, ZnO, and their compositions obtained from XRD.

Chemical composition SnO_2:ZnO	Maximum peak intensity position (2θ) degree	FWHM (2θ) degree	Average crystallite size (D) (nm)
SnO_2	26.6154	0.1338	120.683
70SnO_2:30ZnO	26.5421	0.1224	131.903
40SnO_2:60ZnO	26.6026	0.1020	158.304
30SnO_2:70ZnO	36.2111	0.0816	202.603
20SnO_2:80ZnO	36.2194	0.0816	202.608
ZnO	36.2265	0.1020	162.090

The DTA curves (Figures 2a to 7a) did not show a sharp exothermic peak. This means that the SnO_2, ZnO, and their compositions consist of the crystallized phase, which is also reflected by XRD. Thus the results from DTA are substantiated by the XRD study.

4. Conclusion

The thermogravimetric and differential thermal analysis (TG-DTA) is very useful for investigating the solid-state stability of the ZOTO binary system. It is suitable for use with inorganic materials. The activation energy values from endo and exo DDTA for SnO_2 were |Eg|= 72.06 kJ/g mol and Eg = 325.95 kJ/g mol, respectively. For ZnO they were |Eg|= 40.39 kJ/g mol and Eg = 233.97 kJ/g mol, respectively. In the ZOTO system, endo and exo values of activation energy were |Eg|= 37.34 kJ/g mol and Eg = 254.87 kJ/g mol respectively for mole ratio 40SnO_2:60ZnO. Hence the SnO_2 material absorbs much lower heat (Ea = –72.06 kJ/g mol) compared with ZnO and their compositions. The crystallinity of SnO_2, ZnO, and their compositions from XRD analysis was substantiated by the DTA.

Acknowledgments

The author is thankful to the Head of the Department of Physics, Sant Gadge Baba Amravati University, Amravati, for providing the necessary facilities. Dr SP Yawale, Eminent Professor, is acknowledged for his help in valuable suggestions and discussions.

References

[1] G. Ganguly, D. E. Carlson, S. S. Hegedus, D. Ryan, R. G. Gordon, D. Pang and R. C. Reedy, *Appl. Phys. Lett.*, **85**, (2004), 479.

[2] R. Kaplan and B. Kaplan, *Turk. J. Phys.*, **26**, (2002), 363.

[3] H.-M. Kim, S.-K. Jeung, J.-S. Ahn, Y.-J. Kang, and C.-K. Je, *Jpn. J. Appl. Phys.*, **42**, (2003), 223.

[4] W. Y. Kim, *J. Kor. Inform. Display*, **2**, (2001), 46.

[5] H-S. Goh, R. Adnan and M. A. Farrukh, *Turk. J. Phys.*, **35**, (2011), 375.

[6] T. Minami, T. Miyata and T. Yamamoto, *J. Vac. Sci. Technol.*, **A17**, (1999), 1822.

[7] M. A. Farrukh, B.-T. Heng and R. Adnan, *Turk. J. Chem.*, **34**, (2010), 537.

[8] E. Cetinorgu, S. Goldsmith and R. L. Boxman, *J. Phys. D: Appl. Phys.*, **39**, (2006), 1878.

[9] L. Zheng, Y. Zheng, C. Chen, Y. Zhan, X. Lin, Q. Zheng, K. Wei and J. Zhu, *Inorg. Chem.*, **48**, (2009), 1819.

[10] N. Grioui, K. Halouani, A. Zoulalian, and F. Halouani, *Thermochim. Acta*, **440**, (2006), 23.

[11] M. Raihane, N. Laleque, and B. Boinon, *Thermochim. Acta*, **265**, (2006), 1.

[12] J. D. S. da Silva, C. C. da Silva, L. N. de Lima, A. D. de Oliveira, J. C. O. Santos and A. G. de Souza, *Associacao Brasileira de Analise Termica eCalorimetrica*, (2006).

[13] S. A. Waghuley, *Indian J. Pure & Appl. Phys.*, **49**, (2011), 816.

[14] C. V. Gopal Reddy, W. Cao, O. K. Tan and W. Zhu, *Sens. Actu. B*, **81**, (2002), 170.

[15] G. Zhang, M. Liu, *Sens. Actu. B*, **69**, (2000), 144.

[16] C. N. Xu, J. Timaki, N. Miura, N. Yamazoe, *Sens. Actu. B*, **32**, (1991), 147.

[17] JCPDS data file no. 790205, (1997).

[18] S. A. Waghuley, S. M. Yenorkar, S. S. Yawale and S. P. Yawale, *Sens. Transducers*, **79**, (2007), 1180.

[19] J. Robertson, *Phys. Rev. B*, **30**, (1984), 3520.

[20] S. A. Waghuley, S. M. Yenorkar, S. S. Yawale and S. P. Yawale, *Sens. Actu. B*, **128**, (2008), 366.